Investigating reverse osmosis membrane fouling and scaling by membrane autopsy of a bench scale device

Pablo García-Triñanes, Makrina A. Chairopoulou & Luiza C. Campos

Published online: 04 May 2021.

Submit your article to this journal ⬈

Article views: 18

View related articles ⬈

View Crossmark data ⬈

Investigating reverse osmosis membrane fouling and scaling by membrane autopsy of a bench scale device

Pablo García-Triñanes[a], Makrina A. Chairopoulou[b] and Luiza C. Campos [c]

[a]Materials and Chemical Engineering Group, School of Engineering, University of Greenwich, Gillingham, UK; [b]Department of Process Engineering, TH Nürnberg Georg Simon Ohm, Nuremberg, Germany; [c]Department of Civil, Environmental and Geomatic Engineering, University College London, London, UK
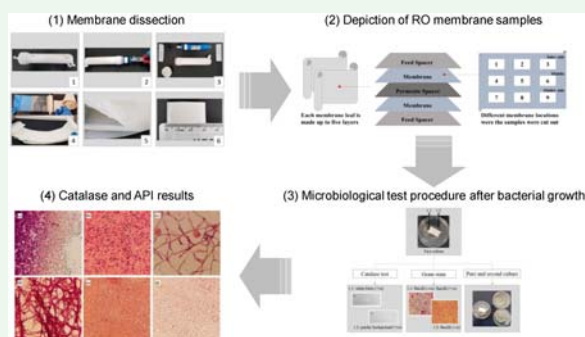
ABSTRACT

In response to the escalating world water demand and aiming to promote equal opportunities, reverse osmosis desalination has been widely implemented. Desalination is however constantly subjected to fouling and scaling which increase the cost of desalination by increasing the differential pressure of the membrane and reducing the permeate flux. A bench-scale desalination equipment has been used in this research to investigate the mitigation of fouling and scaling. This study involved the performance of membrane autopsy for fouling characterisation with special attention to flux decline due to sulphate precipitation and biofouling. Visual inspection, scanning electron microscopy (SEM), energy-dispersive x-ray spectroscopy (EDS), Fourier transform infrared spectroscopy (FTIR) and microbiology tests (API) were performed. Results obtained showed the presence of diatoms, pseudomonas and polysaccharides as the main foulants causing biofouling. Analysis revealed sulphate deposits as well as aluminium, calcium and silica as the main elements contributing to inorganic scaling. Findings pointed out that the pre-treatment system of the small-scale reverse osmosis water treatment was inefficient and that selection of pre-treatment chemicals should be based on its compatibility with the membrane structure. The importance of characterisation for the verification of fouling mechanisms is emphasised.

(1) Membrane dissection   (2) Depiction of RO membrane samples

(4) Catalase and API results   (3) Microbiological test procedure after bacterial growth

Abbreviations and acronyms

AOM	Algal organic matter
API	Analytical Profile Index
ATR-FTIR	Attenuated Total Reflectance Fourier Transform Infrared
BWRO	Brackish water reverse osmosis
SWRO	Seawater reverse osmosis
EDS	Energy-dispersive X-ray spectroscopy
EPS	Extracellular polymeric substances
EPS	Extracellular polymeric substances
GAC	Granular activated carbon
HAOPs	Heated aluminium oxide particles
J	Flux [L/m^{2}h]
NOM	Natural organic matter
RO	Reverse osmosis
SEM	Scanning Electron Microscopy
TDS	Total dissolved solids
ΔP	Pressure drop [Pa]

1. Introduction

Brackish water reverse osmosis (BWRO) and seawater reverse osmosis (SWRO) desalination are processes whereby dissolved solids are removed from a saline water body to produce fresh water.

These solutions have been widely adopted by many countries as a response to the limited fresh water

availability [1–4] with 90 million cubic metres of desalinated water being produced daily in approximately 18,500 desalination plants worldwide [5,6]. The global capacity for seawater desalination amounts to 1.6 million cubic metres per day [7]. BWRO membranes generally allow higher product water (permeate) flux, lower salt rejection and require lower operating pressures (due to the lower osmotic pressures of less saline water), while SWRO membranes require maximum salt rejection at high osmotic pressures. Depending on the water quality, the process can focus on removing monovalent ions, as for example Cl⁻ [8], trace organic chemicals from water streams [9] or crystalline deposits such as $CaSO_4$ [10,11].

Accumulated substances on the membrane surface gradually enhance the boundary layer and create an added resistance. As a result, the total resistance of the membrane increases and the permeate flux (J) decreases based on the following equation:

$$J = \frac{\Delta P}{\mu(R_{BL} + R_m)} \qquad (1)$$

The total resistance is given by the sum of the membrane resistance (R_m) and the resistance of the boundary layer (R_{BL}). ΔP represents the driving force considering the applied pressure discounting the osmotic pressure and μ the viscosity of the solution. Based on the cake filtration model, if the cake continues to grow and is not treated it will cause impaired plant operation and reduce membrane lifetime [12–14].

In cases where the flux decline cannot be explained with the cake filtration model, the obtruding deposit needs to be studied. Particles or microorganisms cause membrane fouling while the reversible or irreversible deposition of salts cause scaling [12,15]. Fouling of an inorganic type is divided in colloidal, when caused by negatively charged particles (clay, silt, proteins and minerals) and in particulate fouling when caused by suspended solids (clay, dirt and sand). In inorganic scaling, known also as precipitation or crystallisation fouling, soluble salts such as calcium carbonate, calcium sulphate, calcium phosphate, barium sulphate and silica precipitate and deposit on the membrane surface when the solubility conditions change. Based on the pH value, inorganic scaling is divided in alkaline ($CaCO_3$), non-alkaline ($CaSO_4$) and silica based when a formation of amorphous silica due to polymerisation takes place. Similarly, organic fouling might be caused by natural organic matter (NOM), wastewater effluent organic matter (EfOM), algal organic matter (AOM) or marine organisms (MO). In NOM, the main foulants are polysaccharides, fatty acids, proteins, amino acids and humic substances. MO and AOM, also referred to as biofouling, are caused by the attachment of living organisms onto the membrane surface. The formed biofilm consists of bacteria and extracellular polymeric substances (EPS). Depending on the type of organism, biofouling is separated into microbiological/microbial when bacteria, algae and fungi are causing the clogging and into macro biological when barnacles and seaweed are observed.

In order to break, loosen or dissolve the accumulated layers and free the membrane's surface, physical and chemical pre-treatment is used [5]. A widely employed method is the use of heated aluminium oxide particles (HAOPs) to remove both NOM and colloids from water and thereby mitigate fouling of membranes [16]. Usually, a step employing ultrafiltration or microfiltration is found efficient to safeguard the membrane. Microfiltration is preferred since it achieves almost the same permeability with less pressure [17]. In some experiments, mechanical vibration was found sufficient to prevent fouling as it changes the hydrodynamics of the system and reduces the concentration polarisation [18,19]. This in turn lowers the permeate flux and prevents cake-enhanced concentration polarisation [18]. Sim et al. [20] suggested online monitoring to decrease fouling by flow diversion and antiscalant dosage regulation by means of installing sensors on the membrane module. In yet another study, the coupling of a granular activated carbon filtration was investigated as a pre-treatment step in a community scale desalination plant with promising results in reducing energy consumption and prevention of biofouling on the membrane [21]. Further strategies include mitigation of fouling by controlling the operating parameters to avoid crystal nucleation [22] or intermittent aeration by using air bubbles as a scrubbing media to minimise fouling on the membrane surface [23]. Despite this first line of defence, foulants and scalants continue finding their way to the RO membrane. In such cases, destructing the membrane cartridges and performing a membrane autopsy is advised to diagnose the type of fouling, identify the foulants and their mechanism and improve the membrane performance and durability by mitigating the obtruding body [24–26].

In this study, we evaluate the fouling and scaling of a bench scale reverse osmosis system by membrane autopsy. The membrane filtration tests were carried out for a duration of three months using raw water from Regent's Park lake, London, and synthetic brackish water. To the authors knowledge this is the first study treating Regent's Park lake water by a reverse osmosis device and represents an original contribution to the study of biofouling considering the accumulation of microorganisms and development of biofilm on the host membranes. This is probably the most arduous

type of fouling providing that the attached substances are living entities.

2. Materials and methods

2.1. Water samples and experimental apparatus

Laboratory tests were performed using 50 L water trolleys of synthetic brackish water and raw water from Regent's Park lake in north-west London, UK. Saline synthetic samples were created using Sodium Chloride CAS: 7647-14-5 (Acros Organics, Avantor) mixed with dechlorinated tap water in a plastic container using a mechanical stirrer to ensure adequate and even mixing (salinity TDS range of 500 mg/L). Pre-treatment was performed with the usage of aluminium sulphate octadecahydrate extra pure CAS: 7784-31-8 (Acros Organics, Avantor). The flocculation process consisted of rapid mixing (400 rpm for 15 s), slow mixing (30 rpm for 20 min) and sedimentation (20 min of settling with no movement into the sedimentation tank). Figure 1 demonstrates the experimental setup that was followed for both water samples.

After the completion of the flocculation, the flocs were removed away from the plastic container and the samples. Regent's Park lake water and subsequently the synthetic brackish water were transferred into the feed tank of the bench scale desalination system for weekly analysis at constant feed temperature of 25°C. Filter cartridges were used to remove particulate matter and avoid materials that could foul the pathways used to remove the RO concentrate. The pre-treatment consists of microfilters (Figure 1(a)), which are membranes with a pore size of 0.1–10 µm and granular activated carbon (GAC) (Figure 1(b)). Permeate from the MF moved on to the GAC filter to further remove organic compounds, chlorine and impurities through chemical adsorption. The feed from the GAC filter passed through the RO membrane to remove bacteria. The retentate (reject water) from the RO membrane returned to the GAC filter. The permeate coming out of the RO membrane proceeded to the post-treatment process consisting of a coconut shell carbon filter. SIP EP2M pump valves were adjusted to ensure that the system is operating at a pressure of 3.5 bar.

RO membranes (Figure 1(c)) are spiral wound polyamide membranes made up of a series of different layers (TW30-1812-100HR; Dow Filmtec^{TM}). The first one is a thin active polyamide layer, the second one is a support layer made of porous polysulfone and this is followed by a thicker reinforcing polyester layer. The active membrane area of the FilmTech RO membrane is found to be 2.782 m^2. The function of the RO membrane is to eliminate dissolved impurities, viruses and bacteria and the design minimum salt rejection is 96%. Coconut shell carbon filter (Figure 1(d)) is used for post-filtration to improve the taste and odour of water. The system has a flow capacity of 50 L/h. For experimental purposes, this system run for 3 h on a five days' basis over a period of three months.

2.2. Autopsy operations

For the purpose of this work, the first and third membranes were removed for autopsy performance. The sequence of the processes carried out is given in Figure 2.

As is shown in Figure 2, the performance of an autopsy test starts by dismantling the RO module from the equipment (1) and by carefully removing the membrane from the casing (2). Next, after placing the membrane on a clean surface (3) it is unrolled while ensuring no smearing or contamination takes place (4). In a further step, the outer wrap, feed spacer and membrane leaves are separated (5) and finally three samples are cut off from each the inlet, middle and outer side of the membrane in 2 × 3 cm pieces for a total of nine samples. Figure 3 depicts the membrane location from where the samples were cut off.

The membrane coupons were analysed according to the procedure outlined in the following sections.

2.3. Inspection and characterisation

Visual inspection is the observation of the physical integrity of the element to visually identify potential foulants. This test was used to help determine what steps to take in thoroughly analysing element performance. The membrane was visually inspected for fouling, defects and damages. Scanning electron microscopy (SEM) analysis at secondary electron imaging mode and low accelerating voltage was used to determine the topography and morphology of the samples (SU8030; Hitachi, Tokyo, Japan). An important advantage of SEM is that the foulants do not have to be removed from the membrane to be analysed. It was evident that the boundary layer had a variable thickness and a changing porosity with deposits growing laterally at places. EDS analysis (10 keV) was used to identify elements present in the sample (SU8030; Hitachi, Tokyo, Japan). Fourier Transform Infrared (FTIR) compares the wavelength of the foulant and scalant found on the surface of the membrane sample against a library of other recorded wavelengths to determine the closest match for identifying the types of chemical bonds present. FTIR spectra were acquired using a Perkin Elmer Spectrum. Recently,
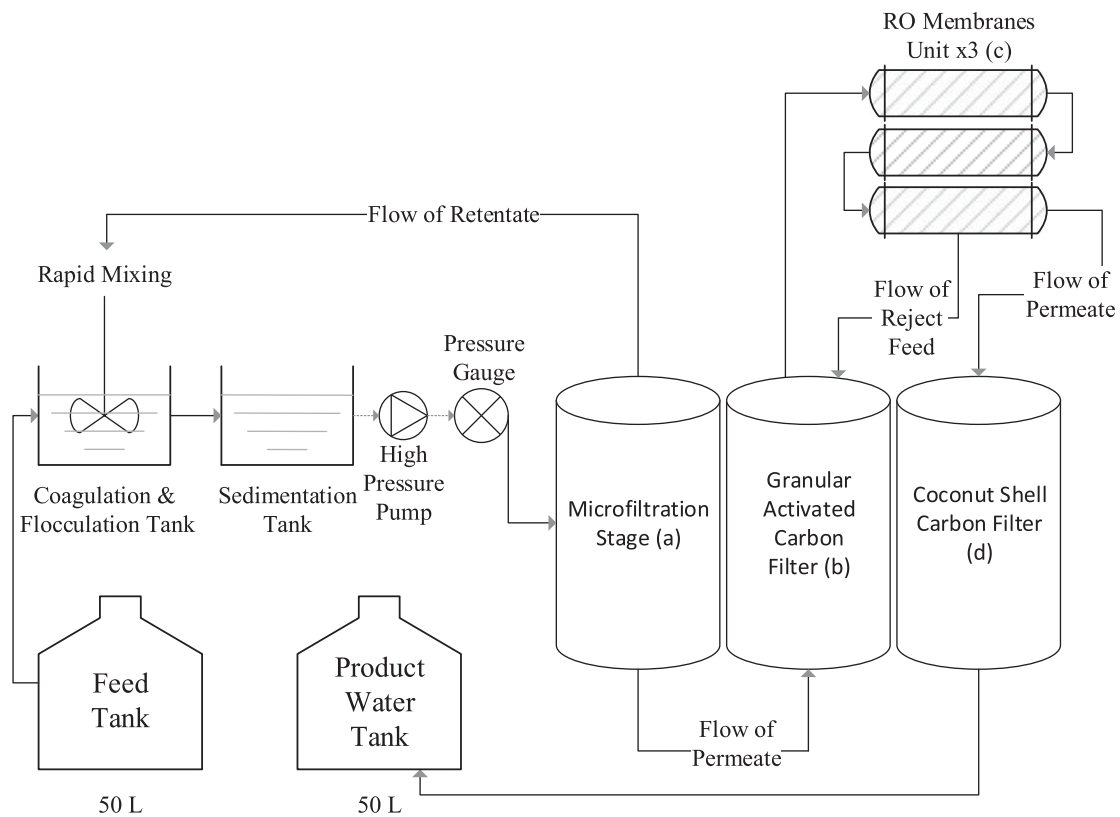
Figure 1. Schematic diagram of the bench scale experimental apparatus.

Raman chemical imaging and ATR-FTIR imaging have proven also advantageous to identify and differentiate inorganic salts on a fouled membrane surface. Both techniques can provide information on the chemical composition of the fouling as well as a high spatial resolution [27].

To identify the type of bacteria causing biological fouling catalase test, gram stain and API (Analytical
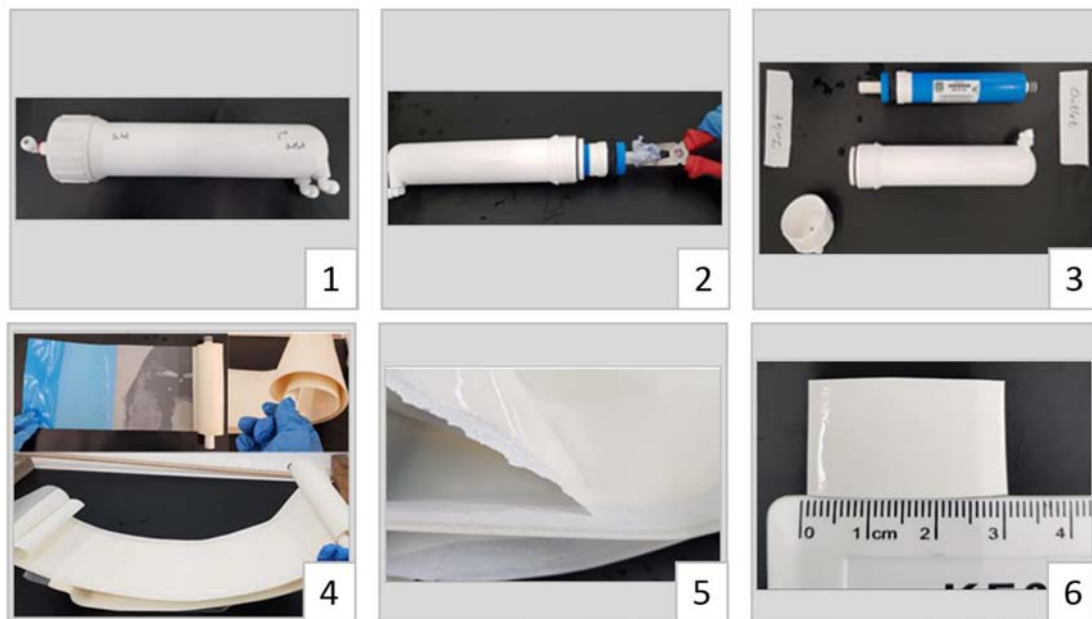
Figure 2. Stepwise description of the membrane dissection carried out to obtain samples required for the performance of membrane autopsy tests.
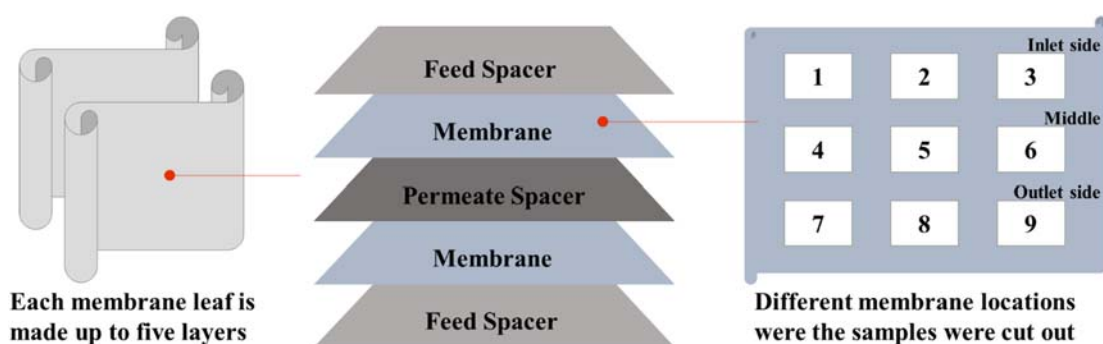
Figure 3. Depiction of RO membrane samples cut out at various positions on the membrane, with the membrane layer located after the feed spacer and two membrane layers separated by the permeate spacer.

Profile Index) test were performed. For the three tests, bacteria present in the membrane were grown in different media culture and conditions listed in Figure 4.

Catalase test is performed to differentiate between aerobic and anaerobic bacteria [28]. Gram stain is then carried out to distinguish between gram-negative and gram-positive bacilli or cocci [29]. Gram-negative bacteria have an outer membrane which makes them resistant to antifouling chemicals and biocides. Gram-positive organisms usually have a thicker and a more tightly adherent layer of peptidoglycans than gram-negative organisms which makes them more resistant to biocide. For this reason, some researchers suggested the use of ultrasonics as an aid technique [30]. API test allows the individual identification of each bacteria, after each colony has been regrown in individual plates to obtain a pure culture [31]. Figure 5 depicts the test procedures.

3. Results and discussion

3.1. Bench-scale water quality after treatment

Table 1 shows the average removal of anions and cations from the RO system.

The results indicate a significant removal of chloride of at least 87% and sulphate of 99% in the product water after treatment by considering average values (iCS-1100 Ion Chromatography System). There is also a high level of removal in nitrate content of about 90%. Furthermore, the results demonstrate that the product water has met the DEFRA UK standards. Figure 6 shows the removal rate of conductivity, salinity and TDS for synthetic NaCl brackish water and raw water with increasing flux. Total Dissolved Solids (TDS) were measured by means of Model 4330 Conductivity and pH Meter.

As is depicted in Figure 6 the removal efficiency of the treatment is relatively high. In the case of synthetic water (NaCl) the removal rate is about 70–99%. For the

Regent's Park lake water sample the tests were performed at much higher permeate flux values ranging from 100 to 320 L/m^2.h. Over time, it also has a consistent removal rate of about 95% which can be used to provide an assessment that this system is effective in treating raw water from Regent's Park lake, London. Likewise, similar trends also indicated that the treatment process can remove up to 85% of hardness (Water Works Total Hardness 481108) from the feed water samples and as the permeate flux increases, the turbidity removal rate still remains high at about 95% (2100AN IS Laboratory Turbidity Meter). The product water has a lower pH (6–8) than the feed water (8–8.5), which is similar to industrial scale systems hence there is also post-treatment. Similarly, the TDS reject concentration has a slight variation with increasing flux. The TDS reject concentration varied from 700 to 1200 mg/L (see Figure 7).

Reject concentration has a slight variation with increasing flux. We postulate that the variation of the RO reject concentration could be caused by the accumulation of residue from previous samples, which resulted in a higher RO reject concentration. This information tells that attention should be paid to the reject as incorrect disposal could result in dire consequences due to its high concentration.

As there was no flushing of the system, the membrane would possibly still contain salts from the previous flow. Occasional high values of the transmembrane pressure indicated the possibility of a dirty or 'fouled' membrane and therefore reduced filtering abilities.

3.2. Fouling analysis

RO membrane fouling was clearly visible as irregularly distributed on some areas of the casing and everywhere over the membrane. The fouling layer was very thin and watery. The feed spacer was however unclogged and without any colour change. Samples
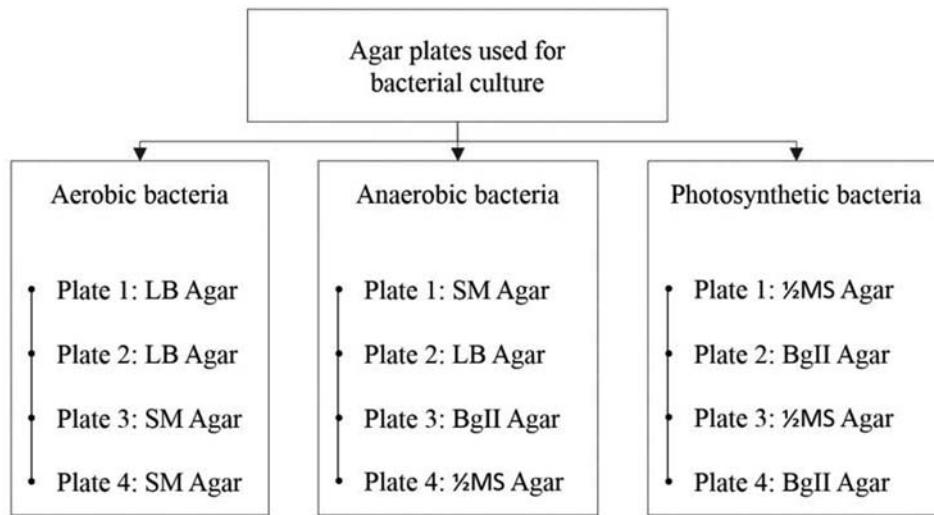
Figure 4. Bacterial culture grown in different types of agar under aerobic, anaerobic and photosynthetic-induced conditions.

of the RO membrane were taken from the first and third RO module at the inlet, middle and outlet side.

Deposit samples were coated with gold prior to SEM analysis. The SEM images showed that different types of diatoms caused biological fouling in both membranes. Salt crystals and deposits were also visible as inorganic scaling. All SEM captures depict a combination of both organic and inorganic fouling. Theoretically, biological fouling would have been expected to be highest in the first membrane and least in the third one due to the direction of feed flow. The reasons for obtaining different results can be due to particle size of foulants being too small or surface chemistry of membrane not being compatible with the water source [32]. Similarly,
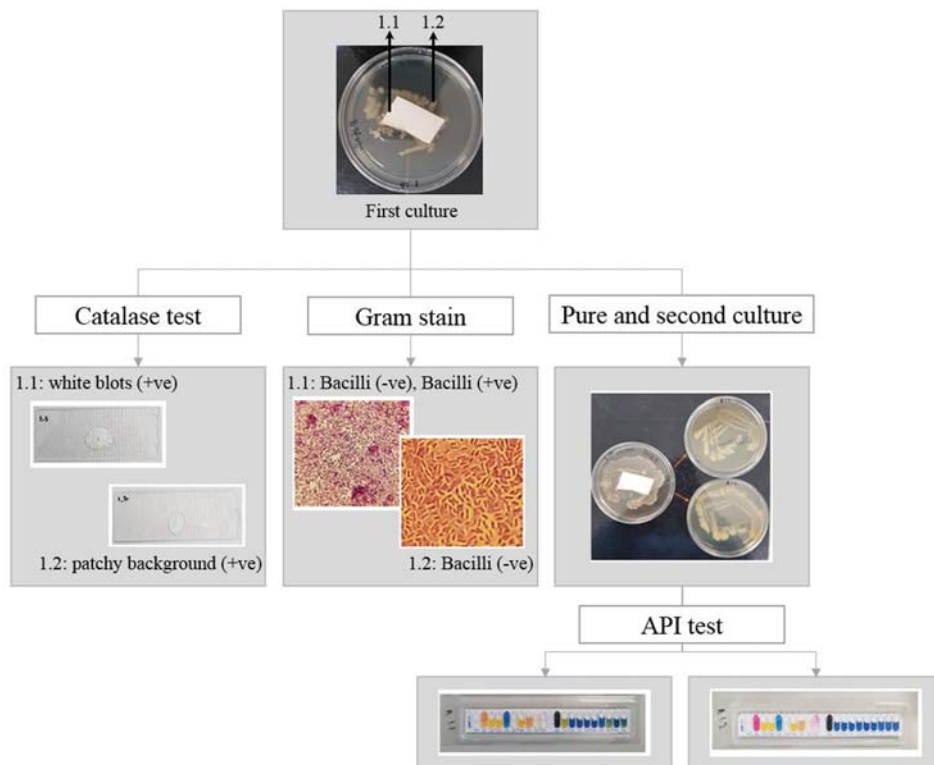
Figure 5. Microbiological test procedure after bacterial growth was visible in the culture media, with catalase test first performed and the occurrence of bubbles indicating catalase-positive bacteria, followed by gram stain to differentiate between bacilli and cocci, and lastly API test for precise identification of bacteria.

Table 1. Average concentration of anions and cations before and after RO treatment.

Samples	Fluoride (mg/L)	Chloride (mg/L)	Bromide (mg/L)	Phosphate (mg/L)	Sulphate (mg/L)	Nitrite (mg/L)	Nitrate (mg/L)
Raw water London Regent's Park	0.85	145.17	0.17	1.25	198.97	N/A	8.78
Product Water from RO treatment system	N/A	18.35	N/A	N/A	2.77	N/A	0.85

scaling would have been expected to be highest in the third membrane compared to the first one due to the increase in concentration of the concentrate upon flowing from first to third membrane in the system. However, results from SEM did not show enough prominent variance to tell the difference. Also, images from the third membrane (Figure 8) show different types of foulants, which did not get filtered by the first membrane. The high level of diatoms deposited on the third membrane show the inefficiency of the first and second membranes to remove most of the biofoulants, and the insufficiency of coagulation and flocculation of the pre-treatment steps.

The composition of the foulants is shown in Table 2 for the first membrane and Table 3 for the third membrane. Based on the SEM and EDS analysis, it was apparent that diatoms were an important cause of fouling. It was also visible that different salt depositions occurred on the third membrane compared to the first one because the water quality of the feed flowing through

the modules change upon flowing from first to third module.

Traces of Mg were also observed in Outlet (2) Pt 3, while Fe was observed in the Inlet (1) Pt 1.

Minor traces of K were observed in Middle (4) Pt 2, Middle (5) Pt 1 and Outlet (2) Pt 2. For both the first and third membranes, the samples show high concentration of O and C suggesting deposits of organic and biological materials. The composition of C varied from 3.7% to 52.2% while that for O varied from approximately 17% to 60% in the first membrane. For the third membrane, percentage of C was up to 49.7% while O was 70.9%. This indicates that diatoms, composed of organic matter, and bacteria were the major components. High percentage of carbon can also appear due to the aromatic functional groups in the polyamide membrane [33]. The presence of sulphur indicates deposits of sulphates that act as physical barriers preventing sorption of water on the membrane surface. Sulphate precipitation affects the performance of the membrane and if kept in solution instead of precipitate the life of the membrane could be prolonged. Of course, an ultimate step to precipitate the SO_4^- using $CaCl_2$ or $BaCl_2$ would be needed to keep the levels of sulphate controlled before discharge according to environmental regulations.

The main elements in the foulants are Na, Al, Si, P, S and Ca. The presence of P is attributed to the presence of bacteria [33]. Substantial amount of Na^+ and Cl^- has also been detected, hence suggesting the deposition of NaCl salts especially at Outlet (2) Pt 1 in the first membrane and Inlet (1) Pt 3 in the third membrane. The appearance of P at various points may be caused by calcium phosphate precipitation. Virgin membrane contains C, O, S, N, Na and Cl [34] which explains the occurrence of N at different points in the third membrane samples. The detection of S can also be due to the polysulfone supporting layer of the membrane [33] originating from building components of the polyamide membrane and polysulfone support.

The presence of Al was mainly due to the aluminium sulphate coagulant used in pre-treatment. The presence of Al was significant at Outlet (2) Pt 3, being up to 10.8%. This means that the coagulant has a strong interaction with the membrane surface or the composition of the membrane. Fernandez-Álvarez et al. [35] suggest the
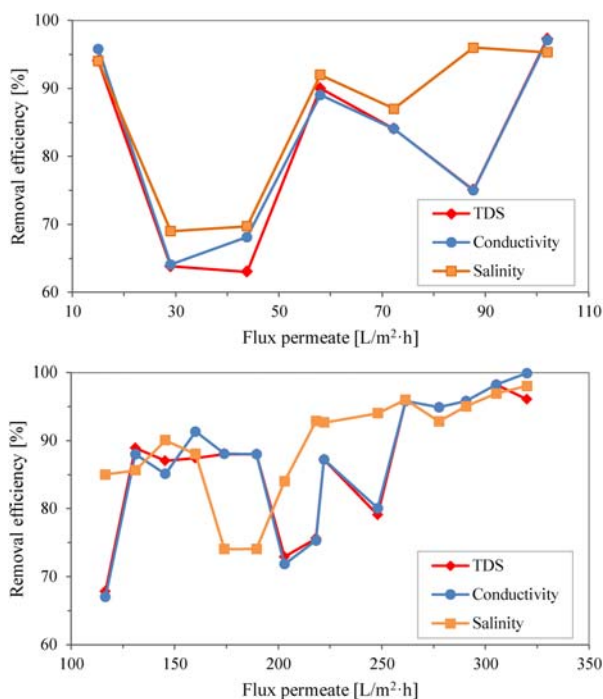
Figure 6. Removal efficiency of conductivity, salinity and TDS against flux permeate for synthetic brackish water (top) and raw water from Regent's Park lake (bottom).
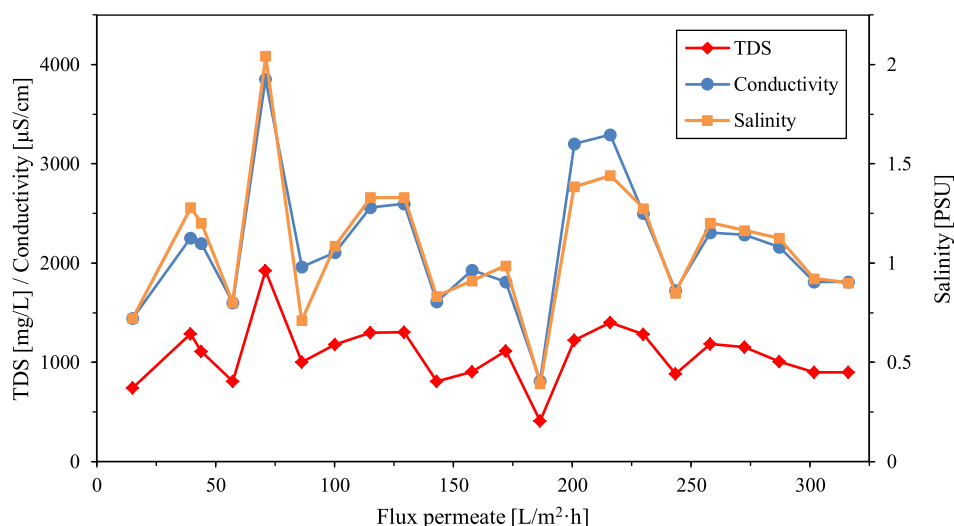
Figure 7. Values of the Conductivity, Salinity and TDS against flux for the Reject.

occurrence of aluminium silicates when Al and Si are present at the same time and these are common foulants in RO operations [36]. Silica scaling is mostly present as colloidal silica [24]. The presence of silicon at various points in the middle and outlet sample indicate colloidal fouling [37].

The percentage of Ca was high at Middle (3) Pt 1 and Middle (4) Pt 1 in the third membrane. The presence of Ca and S indicates that Ca^{2+} and SO_4^- based scaling may be present, the formation of which can be explained by the presence of Fe which has been detected at Inlet (1) Pt 1. The low occurrence of Fe at 2.5 wt% can be related to its natural presence in water. Farhat et al. [38] state that the presence of Fe promotes other types of scaling. It is worth noting that in Tables 1 and 2 the abbreviation Inlet 1.1 corresponds to Inlet (1), Pt 1.

3.3. Fourier transform infrared

The spectrum obtained from the FTIR membrane characterisation is shown in Figure 9. The trivial bands in the range 1500–1600 cm^{-1} are due to the polysulfone support membrane which contain polysulfone groups [39]. They are also associated with the C=C ring vibrations of polyamide. The minor vibrational bands associated with the polyamide layer are the amide group (C=O) near 1712 cm^{-1} and the amine (N-H) near 872 cm^{-1} and they are associated with proteins and polysaccharides biomolecules [40]. The prominent peak at 722 cm^{-1} results due to the presence of aromatic compound [24,36,41].

The peak at 1016 cm^{-1} is characteristic of the functional group C–O and indicates the presence of polysaccharides (constituent of EPS excreted by bacteria). The results obtained through FTIR analysis suggest that the foulants constitute of polysaccharides and aromatic

compounds, which most likely means that a biofilm layer must have developed [32,42].

The band at 970 cm^{-1} indicates the presence of carbohydrate-like substances [37]. The strong absorption peak at 1240 cm^{-1}, originating from the vibration of the P=O bond in nucleic acid, indicates biofouling [43]. The peaks 1240 and 1093 cm^{-1} are also evidence of organic fouling of the RO membrane [33]. According to Jung et al. [23] bands 1712 and 722 cm^{-1} are an indication that irreversible fouling may have been induced and this type of fouling cannot be removed by neither mechanical nor chemical cleaning methods. The presence of inorganic carbonate is evidenced by the peaks at 1341, 872, 847 and 722 cm^{-1} [42].

3.4. Microbiological tests

Microbiological test analyses are summarised in Table 4. All the aerobic bacteria were catalase positive while for the anaerobic bacteria only plates 2.1 and 4.3 were positive. For the photosynthetic culture, bacterial colony in plates 1.4 and 3.2 were positive. The results obtained from the aerobic samples are in line with literature since all aerobes are supposed to be catalase positive. The anaerobes may or may not be catalase positive.

The catalase test was performed as a pre-test to API test, since only catalase-positive bacteria would have given a positive result from the API test. However, in this case the API test was also able to identify the gram-negative bacteria and this is most probably due to bacterial colony contamination. The bacterial colony test samples for catalase and gram stain came from the initial growth culture which was induced in specific agar. The individual bacterial colony used in the API test were however cultured in normal agar due to its
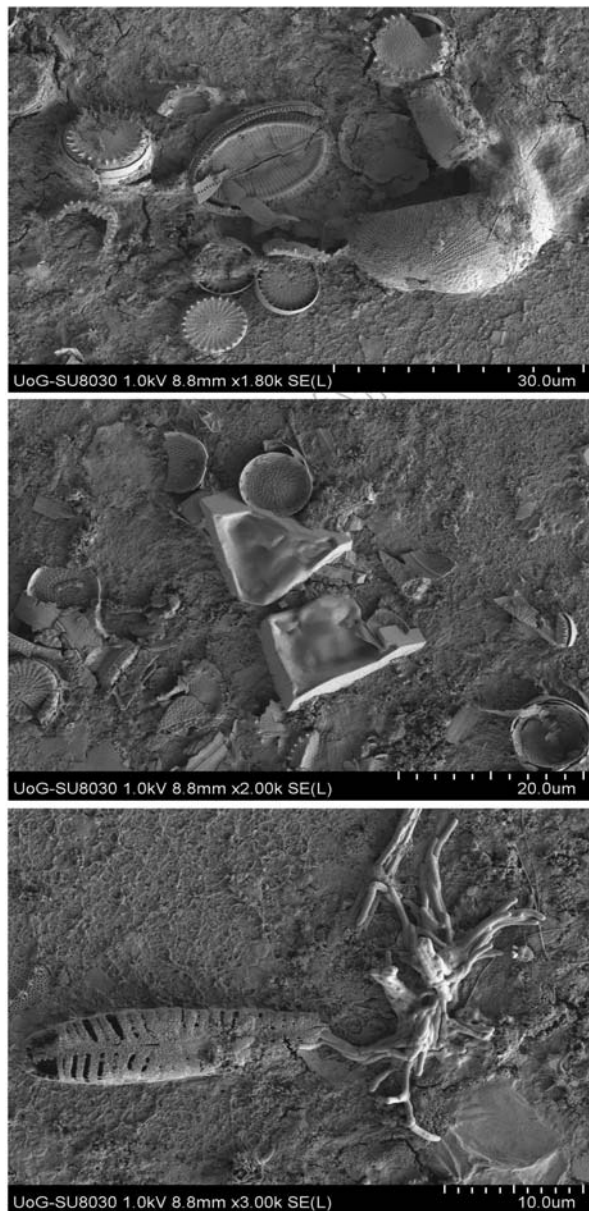
unavailability and time limitation of preparing the specific agar. There is hence a high probability that re-culturing the bacterial colonies separately in a different type of agar may have suppressed the growth of some of the bacteria since the results obtained from the three microbiological tests are not in line with each other. Moreover, the samples which were visible as fungi under microscopic examination, were identified as pseudomonas in the API test, indicating that the agar used in the third test did not support the growth of fungi which initially occurred in the first cultivation.

Samples 4.2, 1.2 and 3.3 were unidentifiable due to the bacterial culture not being pure and getting mixed with other bacteria. Through gram stain of the samples (Figure 10), the aerobic and anaerobic bacteria were identified to be mostly bacilli and the photosynthetic samples as fungi. Performance of the API test enabled more precise identification of the bacteria whereby most of the bacterial colonies from the aerobic, anaerobic and photosynthetic samples were found to be pseudomonas. Some of the pseudomonas are gram-negative implying that they are resistant to antifouling chemicals and biocides.

Pseudomonas and aeromonas which have been identified in this study have also been observed in previous research in RO water treatment [44,45]. Bacteria on the membrane hinder diffusion and decrease osmotic pressure, therefore decreasing the permeate flux. Microbial deposition and EPS excreted by bacteria contribute to the increase in hydraulic resistance near the membrane surface and decrease permeate flux.

4. Final considerations

Synthetic brackish water and raw water were treated by a RO membrane unit. Based on results obtained by accessing parameters such as conductivity, salinity, TDS, pH level and temperature, it was concluded that the reverse osmosis system worked efficiently and met

Figure 8. SEM images of middle samples from the third membrane; (a) radial centric and raphid pennate diatom, (b) crystal deposit and centric diatom and (c) comb-shaped diatom.

Table 2. Fouling analysis at different points on the first membrane showing the percentage elemental composition.

Region	Elements [wt %]									
	C	N	O	Na	Al	Si	P	S	Cl	Ca
Inlet 1.1	12.0	–	32.0	19.8	3.5	–	1.8	–	28.4	–
Middle 1.1	27.8	–	50.8	4.4	5.0	–	3.3	–	5.2	3.5
Middle 1.2	9.0	–	63.7	3.5	3.9	14.0	2.0	–	1.9	1.8
Middle 1.3	24.2	–	53.3	4.8	3.0	10.2	–	–	4.5	–
Middle 1.4	8.9	–	41.1	18.3	3.5	–	1.7	1.7	24.5	–
Middle 1.5	52.2	–	32.1	2.6	–	–	–	9.6	3.5	–
Outlet 1.1	33.6	–	56.8	2.9	1.3	–	0.9	0.3	2.2	2.0
Outlet 1.2	4.2	–	56.8	4.8	2.8	20.4	1.2	1.8	6.5	1.5
Outlet 1.3	4.6	11.1	59.4	2.1	0.3	19.9	–	0.7	1.6	–
Outlet 1.4	18.0	–	51.0	7.6	4.1	3.2	2.3	2.6	9.1	2.2
Outlet 1.5	8.6	–	65.0	4.9	3.6	14.9	–	–	2.9	–
Outlet 2.1	–	–	17.8	30.1	1.6	0.9	0.8	–	48.4	–
Outlet 2.2	21.6	–	54.8	2.5	0.9	13.3	–	3.5	3.4	–
Outlet 2.3	3.7	–	61.2	5.8	10.8	4.7	5.3	–	3.8	4.1

Table 3. Fouling analysis at different points on the third membrane showing the percentage elemental composition.

Region	Elements [wt %]									
	C	N	O	Na	Al	Si	P	S	Cl	Ca
Inlet 1.1	35.7	–	49.8	2.7	1.7	1.4	1.2	–	7.4	–
Inlet 1.2	49.7	–	42.4	1.5	1.3	2.1	0.7	0.7	1.6	–
Inlet 1.3	2.6	–	14.4	31.9	–	–	–	0.5	50.5	–
Inlet 1.4	6.9	–	62.6	4.4	6.5	4.6	3.1	2.2	4.1	2.7
Inlet 1.5	45.2	–	41.6	1.2	–	–	–	10.1	2.0	–
Middle 1.1	2.5	–	14.9	33.4	–	–	–	–	49.2	–
Middle 1.2	39.8	–	49.3	2.9	–	–	–	5.2	2.9	–
Middle 2.1	2.3	–	25.0	23.5	2.5	0.9	1.6	0.8	42.0	1.4
Middle 2.2	5.9	–	15.4	30.1	–	–	–	0.6	48.0	–
Middle 3.1	4.0	–	65.3	0.4	–	–	–	–	0.5	29.7
Middle 4.1	7.1	–	67.7	0.9	–	–	–	0.3	0.5	23.5
Middle 4.2	17.1	22.6	49.6	3.2	1.4	1.3	1.2	0.7	2.5	–
Middle 4.3	17.3	20.0	16.7	1.9	1.9	2.3	1.4	1.6	4.1	1.0
Middle 5.1	15.0	–	59.4	3.6	2.5	14.9	–	1.8	2.2	–
Outlet 1.1	29.6	–	70.4	–	–	–	–	–	–	–
Outlet 1.2	28.8	–	71.2	–	–	–	–	–	–	–
Outlet 2.1	33.2	–	59.5	1.9	–	–	–	3.5	1.9	–
Outlet 2.2	18.2	22.7	52.2	2.4	–	–	0.9	1.1	1.9	–
Outlet 3.1	7.9	–	66.3	2.0	–	19.5	–	2.3	2.0	–
Outlet 3.2	19.2	–	61.4	2.9	–	8.8	–	5.2	2.5	–
Outlet 3.3	24.7	28.2	38.6	1.3	–	–	–	5.0	2.0	–
Outlet 4.1	44.1	–	42.8	1.4	–	–	–	9.7	2.0	–
Outlet 4.2	43.1	–	43.6	1.6	–	–	–	9.6	2.1	–
Outlet 4.3	37.5	–	50.8	1.3	–	–	–	8.4	2.0	–
Outlet 5.1	29.1	–	70.9	–	–	–	–	–	–	–
Outlet 5.2	4.8	–	63.0	4.6	6.8	9.6	3.6	–	4.6	3.0

the standards for drinking water. This complements our previous findings that focused on evaluating a pre-treatment step (coagulation/flocculation) and the permeate quality produced for different influent feed water (data not published). This led us to presume that the pre-treatment step was sufficient and that no fouling or scaling had taken place as the TDS removal efficiency remained high (90%).

This assumption was falsified by membrane autopsy which verified the presence of both foulants and scalants on the membrane surface. SEM and EDS analysis showed Na, Al, Si, P, S and Ca as the main elements and pseudomonas, aeromonas, bacilli and fungi as the major components. Diatoms and bacteria were also identified. The tests suggested a resistance of pseudomonas to antifouling chemicals and biocides while according to FTIR bands (1712 cm^{-1}, 722 cm^{-1}) irreversible fouling took place and was neither possible to restore mechanically nor chemically. Of equal importance to the type of foulant found through autopsy studies is the membrane material itself which should in general display high flux and high rejection [46]. Polyamide membranes used in this study carry a negative charge at the values of pH presented here, so there is inevitably a mutual repulsion between anions and the membrane which can hinder the transport of anions across the membrane. Composite membranes, as the ones studied here, are chemically and physically stable, display a strong resistance to bacterial degradation, do not hydrolyse, are less influenced by membrane

compaction and are stable in a wide range of feed conditions e.g. pH 3–11. However, composite membranes are less hydrophilic and therefore have a stronger tendency for fouling than cellulose acetate membranes [47].

5. Conclusions

Through interpretation of the results several conclusions can be drawn:

- Feed water characteristics were analysed to then deduct foulant type and its physicochemical properties and chemical functional groups in this study.
- Despite the high TDS removal efficiency, membrane autopsy demonstrated biofouling is a dominant mechanism although inorganic foulants and scalants were also present on the membrane surface.
- SEM and EDS analyses showed a high number of diatoms, salt crystals, bacteria and the presence of carbon and oxygen. Although the ratio between inorganic and organic fouling was not deconvoluted in this study.
- The type of inorganic scaling which has been identified include sulphate, aluminium, calcium, silica and carbonate scaling. Aluminium scaling occurred as a result of using aluminium sulphate coagulant. Iron and sodium chloride deposits were also detected through EDS analysis.
- Polysaccharides, which cause irreversible fouling, were identified through FTIR analysis suggesting
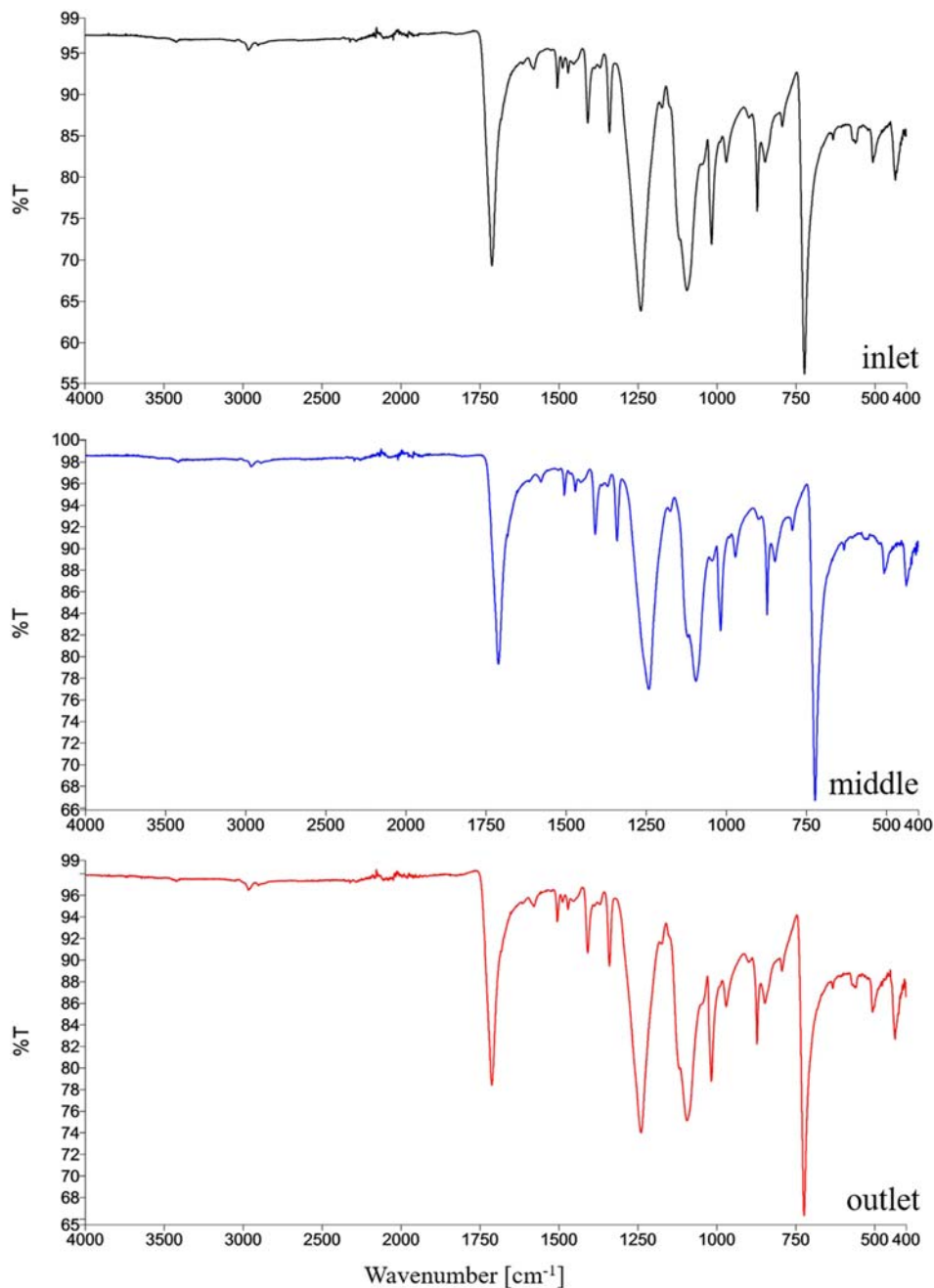
Figure 9. FTIR spectra of membrane for inlet, middle and outlet samples.

that EPS have been produced by the bacteria. Micro-biological tests were used to identify the bacteria as pseudomonas. Numerous and different bacteria have a role in the development of biofilms. Overall, it appeared that mainly pseudomonas and diatoms are the key biofouling organisms.

• Based on the findings of this work, the pre-treatment proved to be inefficient since the microfilters which have the function of removing bacteria, and granular activated carbon which works to eliminate organic chemicals, were not functioning properly or sufficiently. Even though coagulation, which is the main technique to remove diatoms, was used as a pre-treatment, it has proven ineffective. An appropriate selection of biofoulants, coagulant and antiscalant should be made after careful consideration and analysis of the feedwater running through the system. The use of HAOPs will be further investigated as a possible solution to improve the efficiency of the pre-treatment step and reduce fouling.

Future work will hence involve an investigation and redesign of the pre-treatment for the small-scale

Table 4. Catalase test, gram stain and API test results of the aerobic, anaerobic and photosynthetic bacteria grown in different agar culture media.

Bacterial culture	Growth culture	Bacterial Colony	Catalase test	Gram stain bacterial identification	API bacterial identification
Aerobic	1	1.1	+ve	Bacilli (−ve), Bacilli (+ve)	*Pseudomonas oryzihabitans*
		1.2	+ve	Bacilli (−ve)	*Pseudomonas fluorescens*
	2	2.1	+ve	Bacilli (+ve), Bacilli (−ve)	*Pseudomonas oryzihabitans*
		2.2	+ve	Cocci (+ve), Bacilli (−ve)	*Aeromonas salmonicida*
	3	3.1	+ve	Bacilli (+ve), Bacilli (−ve), Cocci (+ve)	*Pseudomonas oryzihabitans*
		3.2	+ve	Bacilli (−ve), Bacilli (+ve)	*Pseudomonas fluorescens*
	4	4.1	+ve	Bacilli (−ve), Cocci (+ve)	*Pseudomonas fluorescens*
		4.2	+ve	Bacilli (−ve)	*Uninterpretable*
		4.3	+ve	Bacilli (−ve), Cocci (+ve)	*Pseudomonas oryzihabitans*
		4.4	+ve	Bacilli (−ve)	*Pseudomonas aeruginosa*
Anaerobic	1	1.1	−ve	Bacilli (−ve), Bacilli (+ve)	*Pseudomonas fluorescens*
	2	2.1	+ve	Bacilli (−ve)	*Pseudomonas oryzihabitans*
	3	3.1	−ve	Bacilli (−ve)	*Pseudomonas oryzihabitans*
	4	4.1	−ve	Bacilli (−ve)	*Aeromonas salmonicida*
		4.2	−ve	Bacilli (+ve)	*Pseudomonas oryzihabitans*
		4.3	+ve	Bacilli (−ve), Cocci (+ve)	*Pseudomonas oryzihabitans*
Photosynthetic	1	1.1	−ve	Filamentous fungi with spores	*Pseudomonas oryzihabitans*
		1.2	−ve	Fungi spores	*Uninterpretable*
		1.3	−ve	Fungi with endospores	*Elizabethkingia meningoseptica*
		1.4	+ve	Filamentous fungi	*Pseudomonas oryzihabitans*
	2	2.1	−ve	Streptococcus bacteria	*Pseudomonas luteola*
	3	3.1	−ve	Filamentous fungi with spores	*Pseudomonas oryzihabitans*
		3.2	+ve	Enterococcus bacteria	*Ochrobactrum anthropi*
		3.3	−ve	Filamentous fungi with spores	*Uninterpretable*
	4	4.1	−ve	Filamentous fungi with spores	*Pseudomonas oryzihabitans*
		4.2	−ve	Spores	*Pseudomonas oryzihabitans*
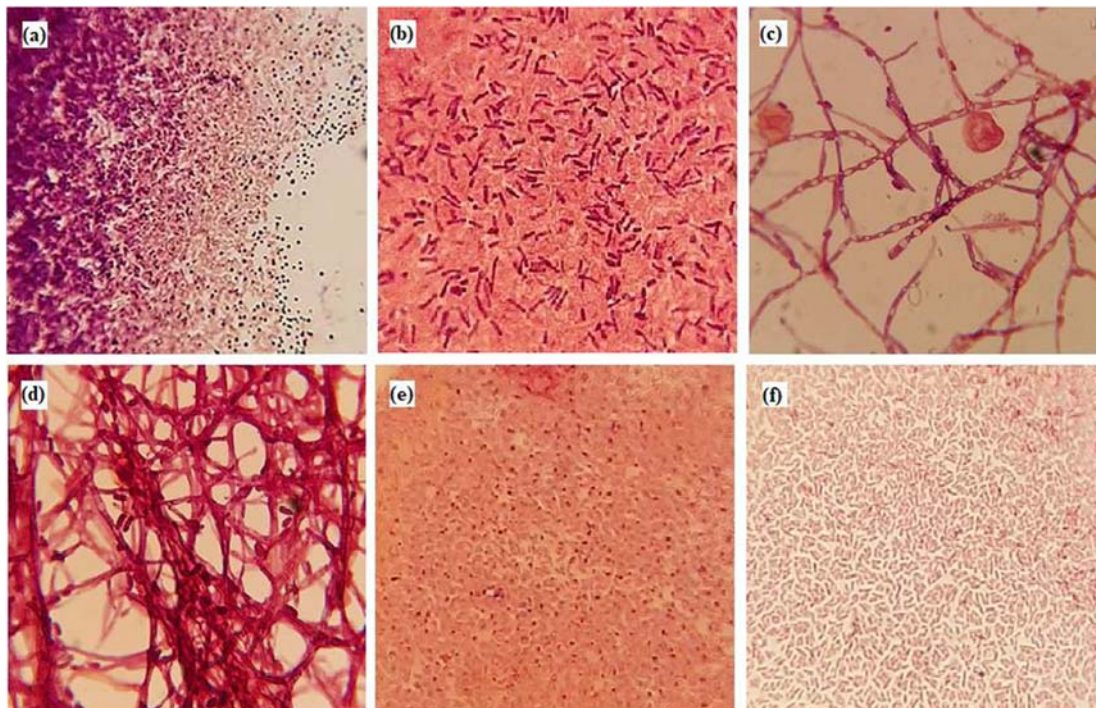
Figure 10. Exemplary sample results obtained through gram stain showing: (a) bacilli positive, bacilli negative and cocci positive for culture 3.1 of aerobic sample; (b) bacilli positive and bacilli negative for culture 1.1 of anaerobic sample; (c) fungi with endospores for culture 1.3 of photosynthetic sample; (d) filamentous fungi for culture 4.1 of photosynthetic sample; (e) bacilli negative and cocci positive for culture 2.2 of aerobic sample; and (f) bacilli negative for culture 2.1 of anaerobic sample.

reverse osmosis system based on these findings with regards to effective treatment for water that has been affected by seawater intrusion.

Disclosure statement

No potential conflict of interest was reported by the author(s).

ORCID

Luiza C. Campos http://orcid.org/0000-0002-2714-7358

References

[1] United Nations. Report of the inter-agency task force on financing for development. New York (NY): United Nations publication; 2018; [cited 2020 Aug 23]. Available from: https://developmentfinance.un.org/iatf2018.

[2] WWAP (United Nations World Water Assessment Programme). The United Nations world water development report 2015: water for a sustainable World. Paris: UNESCO; 2015; [cited 2020 Aug 23]. Available from: https://www.unwater.org/publications/world-water-development-report-2015/.

[3] WWAP (United Nations World Water Assessment Programme). The United Nations world water development report 2017. wastewater: the untapped resource. Paris: UNESCO; 2017; [cited 2020 Aug 23]. Available from: http://www.unesco.org/new/en/natural-sciences/environment/water/wwap/wwdr/2017-wastewater-the-untapped-resource/.

[4] IRENA. (2015). Renewable energy in the water, energy & food nexus. [cited 2020 Aug 23]. Available from: https://www.irena.org/documentdownloads/publications/irena_water_energy_food_nexus_2015.pdf.

[5] International Water Summit. (2018). Energy efficient desalination report. [cited 2020 Aug 24]. Available from: https://www.scribd.com/document/391260972/Energy-Efficient-Desalination-2018.

[6] Zarzo D, Prats D. Desalination and energy consumption. What can we expect in the near future?. Desalination. 2018;427:1–9. doi:10.1016/j.desal.2017.10.046 .

[7] GWI Desal Data/IDA. (2016). IDA desalination yearbook 2016–2017, p. 236.

[8] Malaisamy R, Talla-Nwafo A, Jones KL. Polyelectrolyte modification of nanofiltration membrane for selective removal of monovalent anions. Sep Purif Technol. 2011;77(3):367–374. doi:10.1016/j.seppur.2011.01.005 .

[9] Fujioka T, Hidenobu A, Hitoshi K. Fouling substances causing variable rejection of a small and uncharged trace organic chemical by reverse osmosis membranes. Environmental Technology & Innovation. 2020;17:100576. doi:10.1016/j.eti.2019.100576 .

[10] Gilron J, Hasson D. Calcium sulphate fouling of reverse osmosis membranes: flux decline mechanism. Chem Eng Sci. 1987;42(10):2351–2360. doi:10.1016/0009-2509(87)80109-4 .

[11] John A. B, Johan V, Tzahi Y C. Membrane distillation for concentration of hypersaline brines from the Great Salt Lake: effects of scaling and fouling on performance, efficiency, and salt rejection. Sep Purif Technol. 2016;170:78–91. doi:10.1016/j.seppur.2016.06.028 .

[12] Jiang S, Li Y, Ladewig BP. A review of reverse osmosis membrane fouling and control strategies. Sci Total Environ. 2017;595:567–583. doi:10.1016/j.scitotenv.2017.03.235 .

[13] Boubakri A, Bouguecha S. Diagnostic and membrane autopsy of Djerba Island desalination station. Desalination. 2008;220:403–411. doi:10.1016/j.desal.2007.01.043 .

[14] Goh P, Lau W, Othman M, et al. Membrane fouling in desalination and its mitigation strategies. Desalination. 2018;425:130–155. doi:10.1016/j.desal.2017.10.018 .

[15] Ayoub GM, Korban L, Al-Hindi M, et al. Removal of fouling species from brackish water reverse osmosis reject stream. Environ Technol. 2018;39(6):804–813. doi:10.1080/09593330.2017.1311946 .

[16] Chun Y, Hua T, Anantharaman A, et al. Organic matter removal from a membrane bioreactor effluent for reverse osmosis fouling mitigation by microgranular adsorptive filtration system. Desalination. 2021;506, 115016. doi:10.1016/j.desal.2021.115016 .

[17] Islam Md. S, Touati K, Rahaman Md. S. Feasibility of a hybrid membrane-based process (MF-FO-MD) for fracking wastewater treatment. Sep Purif Technol. 2019;229:115802. doi:10.1016/j.seppur.2019.115802 .

[18] Li W, Su X, Palazzolo A, et al. Reverse osmosis membrane, seawater desalination with vibration assisted reduced inorganic fouling. Desalination. 2017;417:102–114. doi:10.1016/j.desal.2017.05.016 .

[19] Su X, Li W, Palazzolo A, et al. Concentration polarization and permeate flux variation in a vibration enhanced reverse osmosis membrane module. Desalination. 2018;433:75–88. doi:10.1016/j.desal.2018.01.001 .

[20] Sim LN, Chong TH, Taheri AH, et al. A review of fouling indices and monitoring techniques for reverse osmosis. Desalination. 2017;434:169–188. doi:10.1016/j.desal.2017.12.009 .

[21] Monnot M, Nguyên HTK, Laborie S, et al. Seawater reverse osmosis desalination plant at community-scale: role of an innovative pretreatment on process performances and intensification. Chem Eng Process. 2017;113:42–55. doi:10.1016/j.cep.2016.09.020 .

[22] Warsinger DM, Tow EW, Maswadeh LA, et al. Inorganic fouling mitigation by salinity cycling in batch reverse osmosis. Water Res. 2018;137:384–394. doi:10.1016/j.watres.2018.01.060 .

[23] Jung J, Ryu J, Choi SY, et al. Autopsy study of irreversible foulants on polyvinylidene fluoride hollow-fiber membranes in an immersed microfiltration system operated for five years. Sep Purif Technol. 2018;199:1–8. doi:10.1016/j.seppur.2018.01.039 .

[24] Darton T, Annunziata U, del Vigo Pisano F, et al. Membrane autopsy helps to provide solutions to operational problems. Desalination. 2004;167:239–245. doi:10.1016/j.desal.2004.06.133 .

[25] Phuntsho S, Listowski A, Shon HK, et al. Membrane autopsy of a 10 year old hollow fibre membrane from

Sydney Olympic Park water reclamation plant. Desalination. 2011;271(1-3):241–247. doi:10.1016/j.desal.2010.12.040 .

[26] Rautenbach R, Voßenkaul K. Pressure driven membrane processes—the answer to the need of a growing world population for quality water supply and waste water disposal. Sep Purif Technol. 2001;22-23:193–208. doi:10.1016/S1383-5866(00)00130-1 .

[27] Azizighannad S, Intrchomb W, Mitraet S. Raman imaging of membrane fouling. Sep Purif Technol. 2020;242:116763. doi:10.1016/j.seppur.2020.116763 .

[28] PHE. (2019). UK standards for microbiology investigations catalase test. Standards Unit, national infection service, PHE. Bacteriology – test procedures, TP8, Issue no: 4, Issue date: 02.04.19, pp.14. [cited 2020 Aug 24]. Available from: https://assets.publishing.service.gov.uk/government/uploads/system/uploads/attachment_data/file/791639/TP_8i4.pdf.

[29] bioMérieux, Inc. (2008). bioMérieux and Wescor bring a new gram staining instrument for enhanced microbiology laboratory workflow. [cited 2020 Aug 24]. Available from: https://www.biomerieux.com/en/biomerieux-and-wescor-bring-new-gram-staining-instrument-enhanced-microbiology-laboratory-workflow.

[30] Drakopoulou S, Terzakis S, Fountoulakis MS, et al. Ultrasound-induced inactivation of gram-negative and gram-positive bacteria in secondary treated municipal wastewater. Ultrason Sonochem. 2009;16(5):629–634. doi:10.1016/j.ultsonch.2008.11.011 .

[31] bioMérieux, Inc. (2017). API® ID strip range. [cited 2020 Aug 24]. Available from: https://www.biomerieux.co.uk/product/apir-id-strip-range.

[32] Ma H, Hakim LF, Bowman CN, et al. Factors affecting membrane fouling reduction by surface modification and backpulsing. J Memb Sci. 2001;189(2):255–270. doi:10.1016/S0376-7388(01)00422-7 .

[33] Zheng L, Yu D, Wang G, et al. Characteristics and formation mechanism of membrane fouling in a full-scale RO wastewater reclamation process: membrane autopsy and fouling characterization. J Memb Sci. 2018;563:843–856. doi:10.1016/j.memsci.2018.06.043 .

[34] Melián-Martel N, Sadhwani JJ, Malamis S, et al. Structural and chemical characterization of long-term reverse osmosis membrane fouling in a full scale desalination plant. Desalination. 2012;305:44–53. doi:10.1016/j.desal.2012.08.011 .

[35] Fernandez-Álvarez G, Garralón G, Plaza F, et al. Autopsy of SWRO membranes from desalination plant in Ceuta after 8 years in operation. Desalination. 2010;263(1-3):264–270. doi:10.1016/j.desal.2010.06.068 .

[36] Tran T, Bolto B, Gray S, et al. An autopsy study of a fouled reverse osmosis membrane element used in a brackish water treatment plant. Water Res. 2007;41(17):3915–3923. doi:10.1016/j.watres.2007.06.008 .

[37] Karime M, Bouguecha S, Hamrouni B. RO membrane autopsy of Zarzis brackish water desalination plant. Desalination. 2008;220(1-3):258–266. doi:10.1016/j.desal.2007.02.040 .

[38] Farhat S, Bali M, Kamel F. Membrane autopsy to provide solutions to operational problems of Jerba brackish water desalination plant. Desalination. 2018;445:225–235. doi:10.1016/j.desal.2018.08.013 .

[39] Lee W, Ahn CH, Hong S, et al. Evaluation of surface properties of reverse osmosis membranes on the initial biofouling stages under no filtration condition. J Memb Sci. 2010;351(1-2):112–122. doi:10.1016/j.memsci.2010.01.035 .

[40] Chede S, Anaya NM, Oyanedel-Craver V, et al. Desalination using low biofouling nanocomposite membranes: from batch-scale to continuous-scale membrane fabrication. Desalination. 2019;451:81–91. doi:10.1016/j.desal.2017.05.007 .

[41] Yang HL, Huang C, Pan JR. Characteristics of RO foulants in a brackish water desalination plant. Desalination. 2008;220(1-3):353–358. doi:10.1016/j.desal.2007.01.040 .

[42] Sachit DE, Veenstra JN. Foulant analysis of three RO membranes used in treating simulated brackish water of the Iraqi marshes. Membranes. 2017;7(2):23, doi:10.3390/membranes7020023 .

[43] Yu T, Meng L, Zhao QB, et al. Effects of chemical cleaning on RO membrane inorganic, organic and microbial foulant removal in a full-scale plant for municipal wastewater reclamation. Water Res. 2017;113:1–10. doi:10.1016/j.watres.2017.01.068 .

[44] Bereschenko LA, Stams AJM, Euverink GJW, et al. Biofilm formation on reverse osmosis membranes is initiated and dominated by Sphingomonas spp. Appl Environ Microbiol. 2010;76(8):2623–2632. doi:10.1128/AEM.01998-09 .

[45] Sala-Comorera L, Vilaró C, Galofré B, et al. Use of matrix-assisted laser desorption/ionization–time of flight (MALDI–TOF) mass spectrometry for bacterial monitoring in routine analysis at a drinking water treatment plant. Int J Hyg Environ Health. 2016;219(7, Part A):577–584. doi:10.1016/j.ijheh.2016.01.001 .

[46] Kavaiya AR, Raval HD. Highly selective and antifouling reverse osmosis membrane by crosslinkers induced surface modification. Environ Technol. 2021, 1–12. doi:10.1080/09593330.2020.1869316.

[47] Zhao S, Huang G, Cheng G, et al. Hardness, COD and turbidity removals from produced water by electrocoagulation pretreatment prior to reverse osmosis membranes. Desalination. 2014;344:454–462. doi:10.1016/j.desal.2014.04.014 .